

Effect of Glycerol Addition on Copper Electrodeposition on Steel Substrate

Rafael Santos Barbosa^a , Guilherme Yuuki Koga^b, Marcio Luis, Ferreira Nascimento^a ,

Carlos Alberto Caldas de Souza^{a,*} 

^aUniversidade Federal da Bahia, Escola Politécnica, Programa de Pós-Graduação em Engenharia Industrial, Rua Aristides Novis, 2, Federação, 40210-630, Salvador, BA, Brasil.

^bUniversidade Federal de São Carlos, Departamento de Engenharia dos Materiais, Rod. Washington Luis, km 235, 13565-905, São Carlos, SP, Brasil.

Received: January 13, 2022; Revised: April 24, 2022; Accepted: May 30, 2022

This work investigates the effect of the addition of glycerol on the microstructure, corrosion resistance, and efficiency of the electrodeposition process of Cu coating in an acid sulphate solution. The morphology and microstructures of electrodeposits were analyzed using Scanning Electron Microscopy (SEM), Spectrometry X-Ray Diffraction (XRD) and laser scanning confocal microscopy (LSCM). Evaluation of the corrosion resistance was performed in 2.0 mol·L⁻¹ NaCl by means of weight loss tests and electrochemical techniques. The addition of glycerol resulted in a decrease in grain and crystallite sizes, a decrease in roughness and an increase in the tensile strain of the coating. The deposition efficiency and the corrosion resistance increased with the addition of glycerol exhibiting a maximum value at the concentration of 0.42 mol·L⁻¹, increasing the efficiency of electrodeposition by approximately 96%. This is related to the roughness of the coating, which is minimal at this concentration.

Keywords: Cu coating, glycerol, electrodeposition, corrosion.

1. Introduction

Copper coatings obtained through electrodeposition have been widely used given their high conductivity, which is useful for several industrial sectors such as electronics, automotive, and aerospace industries¹. Various types of electrolyte solutions including alkaline cyanide² and non-cyanide (acid sulfate and pyrophosphate)^{3,4} bath can be used for electrodeposition. Copper electrodeposition using cyanide solutions is an industrial practice that obtains deposits with excellent brightness and adhesion. However, the high toxicity of cyanide solutions generates considerable costs with the treatment of effluents and poses safety risks for workers².

Deposition of copper from aqueous sulphuric acid containing copper sulfate is widespread in industry due to the speed of the electrodeposition process, the relatively low cost, and the ease of control and maintaining the electrodeposition⁵. Furthermore, it is possible to obtain uniform, ductile, and strong coatings². Copper coatings obtained from an acid sulphate solution have been used in various devices and equipment such as printed circuit boards and semiconductors⁶, musical instruments, heat exchangers, reflectors⁷, and in a permanent mold with 15 μm of electrodeposited copper for closing cavities, pores or cracks in steel surfaces⁸.

A good quality copper coating must be smooth and dense, and no nodules and dendrite formation should occur⁹, favoring the coating's resistance to corrosion. The effect of adding various additives to the copper bath has been investigated to obtain coatings with these characteristics and to increase the efficiency of the electroplating process.

Regarding sulphuric plating baths, the effect of additives such as thiourea^{9,10}, gelatin⁹, benzotriazole^{5,11,12}, DPS (3-N,N-dimethylaminodithiocarbamoyl-1-propanesulphonic acid) and PEG (polyethylene glycol)¹³ have been studied.

Thiourea and benzotriazole are among the most studied additives in relation to Cu deposition through a sulfate plating bath. These additives are adsorbed on the Cu coating resulting in a refining of grains and in a smoother coating, favorable to corrosion resistance. Thiourea adsorption occurs by bonding the sulphur atoms of this molecule and copper¹⁰, while benzotriazole adsorption occurs through the interaction of the nitrogen atoms of this molecule with the substrate and copper ions¹¹. It has been reported⁹ that thiourea has a synergetic effect with gelatin, and the joint addition of these additives results in a deposit with less roughness and an absence of pores and nodules. A joint effect of additives in decreasing the roughness of the copper coating is also found with the addition of DPS and PEG, and also a decrease in the resistivity of the coating has been reported¹³.

About organic compounds added to the electrodeposition bath, it has been reported that glycerol, which is environmentally friendly, when added to the electrodeposition of various metals and alloys results in a beneficial effect^{14,15}. Regarding Cu deposition, it has been found¹⁶ that the addition of glycerol to an alkaline copper deposition bath complexed with pyrophosphate decreases the porosity and micro-strain of the coating. Furthermore, the addition of glycerol inhibits hydrogen evolution in copper electrodeposition processes, improving the allowable current density, but decreasing the current efficiency.

*e-mail: caldassouza@ufba.br

The complexation of copper ions with glycerol results in a uniform smooth coating with body centered cubic structure¹⁷. It has been suggested that in an alkaline bath in the presence of glycerol, the complex $\text{Cu}_2(\text{OH})(\text{glyc})^{2+}$ is formed, which is dissolved with NaOH resulting in the formation of the complexes $\text{Cu}(\text{glyc})$ and $[\text{Cu}(\text{glyc})_2]^{2-}$ which are thermally more stable than the $\text{Cu}^{2+}/\text{OH}^-$ complex¹⁸.

Unlike the Cu coating obtained through alkaline bath, it is not clear how the addition of glycerol affects the characteristics and the corrosion resistance of the coating obtained through acid sulfate bath. In the present paper, the electrodeposition of copper on AISI 1020 steel substrates was evaluated from acid sulphate solution in the presence and absence of glycerol. The effect of anions of glycerate and sulfate on the morphology of the copper electrodeposits and their corrosion resistance were assessed. The findings contribute to a better understanding of Cu-coatings by electron deposition to protect the surface of carbon steel against corrosion in a sustainable way.

2. Experimental Procedure

We present the best electrodeposition conditions for a deposition bath as well as other experimental procedures regarding copper morphology and structure, deposition efficiency and evaluation of corrosion resistance.

2.1. Deposition bath and electrodeposition conditions

The composition of the copper electroplating bath is listed in Table 1. The following concentrations of glycerol were added to the bath: 0.14, 0.28, 0.42 and 0.56 mol·L⁻¹. The addition of amounts of glycerol greater than 0.856 mol·L⁻¹ resulted in a non-adherent coating to the substrate.

Before each galvanostatic electrodeposition, the pH and conductivity of the copper deposition baths were measured in the absence and presence of glycerol, at room temperature (~25 °C), as shown in Table 2. The pH and conductivity values of the Cu coating electrodeposition baths were obtained in the absence and presence of different glycerol concentrations

Cu coatings were electrodeposited onto a carbon steel AISI 1020 substrate embedded in a polymeric resin. The parameters used in the galvanostatic deposition were: room temperature (25 °C), without agitation, current density 10 mA·cm⁻², graphite bar used as anode, electrodeposition time 22 min and 30 s, to reach a 5 μm thick coating determined by Faraday's law.

2.2. Morphology and structure

The morphology of Cu coatings were studied using a scanning electron microscope (SEM, JSM - 6610LV, brand JEOL) equipped with energy dispersive X-ray spectrometer

(EDS) with 500× and 3,000× magnification. Through SEM micrographs, the mean size and density of the grains were determined¹⁹. These measurements were obtained using ImageJ software, version 1.53e, with 3,000× magnification micrographs. An example of using the software can be seen in the Supplementary material.

The surface roughness of the Cu film was measured by laser scanning confocal microscopy (LSCM) using the Olympus model LEXT OLS4100 equipment. The measurement observation field was 256 μm × 256 μm. Through roughness measurements, the following parameters were obtained: S_a (arithmetic mean of the absolute value of roughness within a defined area), S_q (mean squared deviation of roughness, corresponding to the standard deviation of heights), S_p (Maximum height between the peaks highest and midplane) and S_v (Maximum depth between midplane and deepest valley).

The parameter S_a was determined through the following Equation 1²⁰:

$$S_a = \frac{1}{A} \iint_A |z(x, y)| dx dy \quad (1)$$

where A represents the defined scanning (or observation) area, and x , y , and z correspond to the coordinates of length, width, and height, respectively.

The structure of Cu coatings was analyzed using X-ray diffraction (XRD) in a SHIMADZU model XRD-6000 diffractometer, with Cu-K α radiation (40 kV and 40 mA). From the XRD diffractograms, the relative texture coefficient (T_c), the crystallite size, and the microstrain of Cu coating were determined.

The texture coefficient (T_c) was obtained through the following Equation 2²¹:

$$T_c(hkl) = \frac{I(hkl) / I_0(hkl)}{\frac{1}{n} \sum I(hkl) / \sum I_0(hkl)} \quad (2)$$

where $I_{(hkl)}$ is the reflection intensity of an experimentally measured crystal plane, $I_{0(hkl)}$ is the reflection intensity for a crystal plane of a standard copper sample (International Center for Diffraction Data - ICDD), and n is the number of peaks present in the diffractogram.

The crystallites size of the Cu coating were obtained using the Scherrer Equation 3²²:

$$d = \frac{k\lambda}{(\beta_l \cos \theta)} \quad (3)$$

where d is the crystallite size; λ is the wavelength of the element used for the diffraction, β_l is a full width at half maximum (FWHM), and θ is the corresponding angle.

The microstrain of Cu coating was determined using the method of Williamson and Hall²³ using the following Equation 4:

Table 1. Summary of concentrations and function in the electrolytic bath.

Chemicals	Concentrations	Function
Sulfuric acid (H ₂ SO ₄)	0.5 mol·L ⁻¹	Supporting electrolyte
Sodium sulfate (Na ₂ SO ₄)	1.0 mol·L ⁻¹	Background electrolyte
Copper (II) sulfate (CuSO ₄ ·5H ₂ O)	0.8 mol·L ⁻¹	Source of Cu ²⁺ ions
Sodium chloride (NaCl)	40 mg·L ⁻¹	Source of Cl ⁻ ions

Table 2. Lists of pH and conductivity values of the Cu coating electrodeposition baths obtained in the absence and presence of different concentrations of glycerol.

Sample	Glycerol concentration (mol.L ⁻¹)	pH	Conductivity (mS.cm ⁻¹)
1	0	0.50	364.5
2	0.14	0.60	359.5
3	0.28	0.68	357.5
4	0.42	0.74	354.7
5	0.56	0.80	351.8

$$\beta_{hkl} \cos \theta = \frac{K\lambda}{d} + 4\epsilon \sin \theta \quad (4)$$

where ϵ is the microstrain, d is the interplanar distance, K is the shape parameter which is 0.94 for spherical shape.

The nature of the microstrain of Cu coating was determined by obtaining the Williamson-Hall plot ($\beta_{hkl} \cos \theta$ vs. $4 \sin \theta$). The lattice strain has a positive slope when the crystal lattice experiences tensile forces whereas lattice shrinkage due to the compressive strain was indicated by the negative slope, but the horizontal slope indicates a crystal free of any microstrain^{24,25}.

2.3. Deposition efficiency

The galvanostatic deposition efficiency percentage (E)²⁶ was evaluated by the ratio between the copper electroplated mass and the theoretical mass (Equation 5):

$$E (\%) = \frac{[1 - (m_c - m_r)] \cdot 100}{m_c} \quad (5)$$

where m_r is the measured Cu mass gain, and m_c is the theoretical mass gain, calculated by Equation 6:

$$m_c = \frac{t_i \cdot M_i \cdot I}{n_i C_i F} \quad (6)$$

where t_i is the deposition times (second), I is the total current passed (amperes), n_i is the number of electrons transferred per atom of metal, C_i is the weight fraction (1 to Cu coating), M_i is the atomic mass of that element (g.mol⁻¹), and F is the Faraday's constant.

Using Faraday's law, m_c is related with the thickness of the coating by Equation 7²⁷:

$$t_h = \frac{m_c}{D_i S_A} \quad (7)$$

where t_h is the film thickness, (5 μ m); D_i is the Cu density (g.cm⁻³) and S_A is the electrodeposition surface (2.01 cm²).

Energy consumption (kwh/ton), E_C was calculated by using the Equation 8²⁸:

$$E_C = \frac{V_m 8.4 \times 10^5}{10C_E} \quad (8)$$

where V_m is the average potential (in V) and C_E the current efficiency percentage (in %).

2.4. Evaluation of corrosion resistance

Corrosion resistance was evaluated in 2.0 mol.L⁻¹ NaCl solution, through measurements of mass loss and electrochemical

techniques. In the measurements of mass loss, the deposits obtained in the absence and in the presence of different concentrations of glycerol were considered. All values were obtained in triplicate submitted to a 24 h immersion time with substrate area of 2 cm² fully exposed to the corrosive solution. The cleaning of the surface of the Cu coating after immersion in a corrosive solution was done with a solution of glycine (aminoacetic acid - C₂H₅O₂N) 1.36 mol.L⁻¹ at room temperature. Through mass loss measurements the corrosion rate (C_R), expressed in mm per year, was calculated using the following Equation 9²⁹:

$$C_R = \frac{K_C W}{A \cdot t_e D_i} \quad (9)$$

where K_C is a constant (for C_R mm/year, $K_C = 8.76 \times 10^4$); W is the mass loss (g); A is the exposed area (cm²); t_e is the duration of exposure (h); D_i is the Cu density (g.cm⁻³).

Electrochemistry test system (AUTOLAB potentiostat/galvanostat model PGSTAT100, controlled by NOVA 1.11 software) containing a conventional three-electrode cell was applied to carry out potentiodynamic polarization tests. A saturated calomel electrode (SCE) as a reference electrode and graphite as counter electrode were used. Samples were kept in the electrolyte for 30s before performing electrochemical experiments. The potentiodynamic polarization curves were recorded at a scan rate of 10 mV.s⁻¹, and from these curves, polarization resistance, R_p , and corrosion current density, i_{cor} , were obtained.

The polarization resistance was obtained through the potentiodynamic comparison curve of E (potential) vs i (current density) and corresponds to the inverse of the slope of the tangent line to the overpotential of 10 mV vs. SCE. The i_{cor} values were obtained through the E vs. $\log i$ polarization curve (Tafel curve) using the linear polarization method based on the Stern-Geary Equation 10³⁰.

$$i_{cor} = \frac{b_a b_c}{3.2 R_p (b_a + b_c)} \quad (10)$$

where i_{cor} is the corrosion current density, R_p is the polarization resistance (in Ω), b_a is the anodic Tafel slope, and b_c is the cathodic Tafel slope.

3. Results and Discussion

3.1. Effect of the addition of glycerol on the morphology and size grain of the Cu coating

Figure 1 shows the SEM micrographs of Cu coating obtained in the absence (Figure 1a) and the presence (Figure 1b, c, d, e) of different amounts of glycerol. Table 3 shows the mean grain size and grain population density values obtained from SEM micrographs. These micrographs revealed the presence of evenly distributed nodular grains. The addition of glycerol did not change the shape of the grains, however, it caused a decrease in the average grain size. Furthermore, the addition of glycerol made the coating more uniform causing an increase in the population density of copper grains. The reduction in grain size is related to the effect of adding glycerol on the size of the crystalite, and this effect is discussed in item 3.2. The effect of grain refining caused by the addition of glycerol in bath deposition was also verified

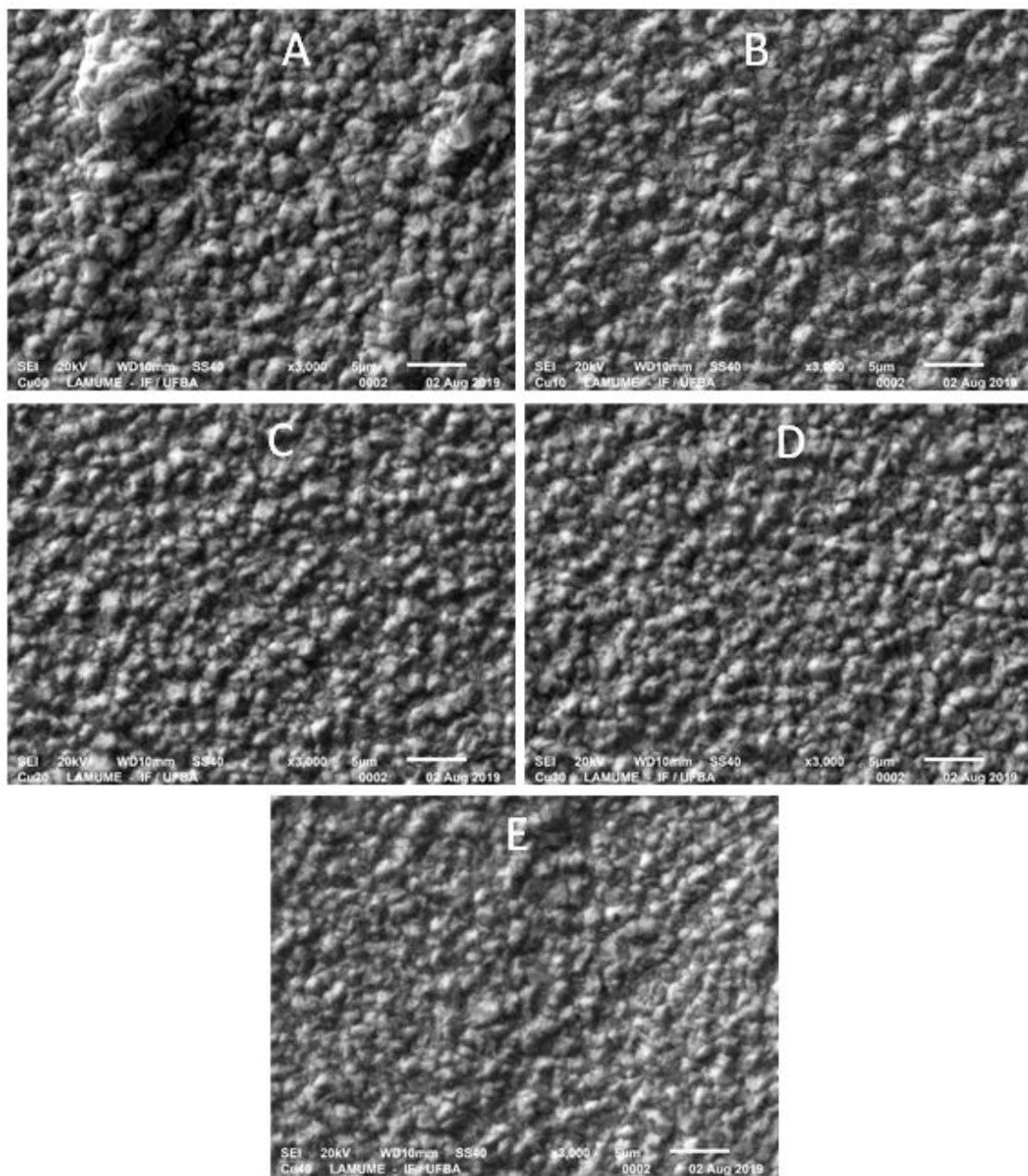


Figure 1. SEM micrographs of Cu coating obtained in the presence (*b, c, d, e*) and absence (*a*) of different glycerol contents. (*b*) $0.14 \text{ mol}\cdot\text{L}^{-1}$, (*c*) $0.28 \text{ mol}\cdot\text{L}^{-1}$, (*d*) $0.42 \text{ mol}\cdot\text{L}^{-1}$, (*e*) $0.56 \text{ mol}\cdot\text{L}^{-1}$.

Table 3. Effect of glycerol addition on average grain size and population density of grains of Cu coating in the absence and presence of different glycerol concentrations.

Glycerol concentration ($\text{mol}\cdot\text{L}^{-1}$)	Mean value of the grain size (μm)	Mean value of the population density of the grains ($\text{grains}/\mu\text{m}^2$)
0	3.2 ± 0.07	0.32 ± 0.008
0.14	2.9 ± 0.07	0.37 ± 0.008
0.28	2.7 ± 0.07	0.45 ± 0.008
0.42	2.4 ± 0.07	0.55 ± 0.008
0.56	2.3 ± 0.07	0.61 ± 0.008

in Zn coating¹⁴ and Zn-Ni coating¹⁵, in addition to Cu-Zn-Sn coating³¹, and Cu coating¹⁷, obtained from alkaline baths.

3.2. Evaluation of the addition of glycerol on the physical structure of the copper coating

Figure 2 shows the diffractograms obtained for Cu coatings obtained in the absence and presence of varying concentrations of glycerol. The XRD pattern of Cu coatings in Figure 2 exhibits the planes (111), (200), and (220), which correspond to Cu, and the plane (110) that corresponds to Fe from the steel substrate¹⁷. In these diffractograms, the

presence of diffraction peaks characteristic of the crystalline structure can be observed. Even after the addition of glycerol in the bath deposition, the peaks indicate that the crystalline structure of the copper coating was maintained. This shows that the increase in the carbon content in the coating resulting from the addition of glycerol was not enough to cause the amorphization of the structure of the copper coating.

In order to evaluate the effect of glycerol addition on the orientation of the Cu coating planes, the texture coefficient was determined from the XRD pattern. The orientation with maximum texture coefficient is the preferential orientation of the coatings. Therefore, the texture coefficient (T_c) values, shown in Table 4, indicate that the copper coating deposited both in the absence and in the presence of glycerol has as preferential orientation the plane (220). However, Hu et al.¹⁶ found that the addition of $0.04 \text{ mol}\cdot\text{L}^{-1}$ of glycerol to the alkaline pyrophosphate-based copper deposition bath changed the preferential orientation from the plane (220) to the plane (111). In an alkaline copper bath complexed with glycerol, it was found¹⁸ that the deposited coating has plane (111) as the preferred orientation, which was not changed with the addition of additives such as gelatin, anisaldehyde, imidazole and peptone. These results therefore show that the crystallographic texture of the copper coating, as well as the effect of the additive on the texture, depend on the composition of the bath and on the conditions of the electrodeposition.

The fact that the texture coefficient of the preferred orientation plane is greater than 1 ($T_c(220) > 1$) indicates a high crystallinity of the copper film³². The decrease in the T_c of the plane (220) with the addition of $0.56 \text{ mol}\cdot\text{L}^{-1}$ of glycerol may be related to a decrease in the crystallinity of the deposit caused by the increase in the carbon content.

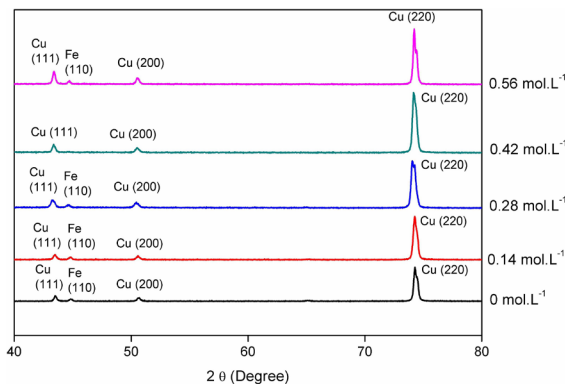


Figure 2. XRD pattern for Cu coatings obtained in the absence and presence of different glycerol concentrations related to JCPDS 89-2838.

However, as can be seen from Table 2, there is no clear trend as to how the addition of glycerol affects T_c .

From the XRD pattern shown in Figure 2, the mean crystallite size values were also obtained, using the Scherrer equation²², as well as the microstrain values, determined by the Williamson-Hall formula²³, which are described in Table 3. The crystallite size values are consistent with the values found by Sekar et al.¹⁷ in a Cu coating obtained using an alkaline bath and values between 25.59 and 32.06 nm were found.

The results listed in Table 5 show that the size of the copper crystallites decreases, while the microstrain increases with the addition of glycerol. This inverse relationship between the average crystallite size and microstrain has also been noted in the literature²¹. In Table 5 nanometer copper crystallites with an average of 30 nm can be seen.

The observed reduction in crystallite sizes due to additives generally implies a decrease in grain sizes, which was observed in the present work considering glycerol (Table 5). It is possible that this addition has the effect of shifting the deposition potential in the cathodic direction, which reduces the energy of nucleus formation, resulting in an increase in the nucleation rate, and consequently in the refining of the grains³².

Figure 3 shows the Williamson-Hall plot, which is used to determine the nature of the coating's microstrain. The positive slope of this graph indicates a network traction, while the negative slope indicates a network compression, but the horizontal slope indicates a crystal free from any microdeformation^{23,24}. Therefore, Figure 3 indicates that the nature of the deformation present in copper deposits is tensile. Thus, by increasing the microstrain, the addition of glycerol favors the increase in the Cu coating's tensile

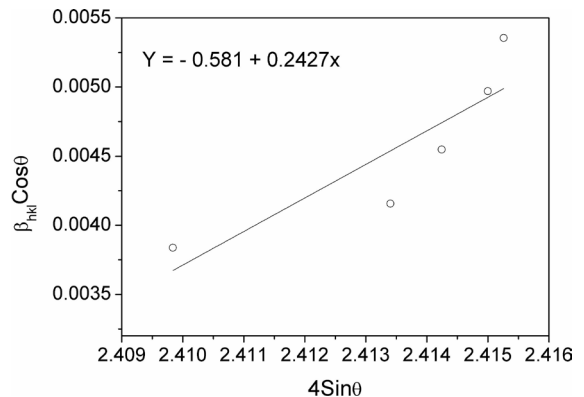


Figure 3. Williamson-Hall plot used to analyze the microstrain nature of copper coating in the absence and presence of glycerol.

Table 4. Copper coating texture coefficient, in the absence and presence of different concentrations of glycerol.

Plan (hkl)	T_c without glycerol	T_c with $0.14 \text{ mol}\cdot\text{L}^{-1}$ glycerol	T_c with $0.28 \text{ mol}\cdot\text{L}^{-1}$ glycerol	T_c with $0.42 \text{ mol}\cdot\text{L}^{-1}$ glycerol	T_c with $0.56 \text{ mol}\cdot\text{L}^{-1}$ glycerol
111	0.18	0.13	0.18	0.15	0.25
200	0.27	0.23	0.27	0.21	0.31
220	8.17	8.59	8.06	8.62	7.69
311	0.39	0.36	0.53	0.29	0.35

Table 5. Average size of copper crystallites and microstrain in the absence and presence of different concentrations of glycerol.

Glycerol concentration (mol·L ⁻¹)	Average size of copper crystallites (nm)	Microstrain values of crystalline copper (%)
0	35.3	0.16
0.14	32.6	0.17
0.28	29.8	0.19
0.42	27.3	0.21
0.56	25.3	0.22

stress. However, the effect of glycerol on the microstrain of the copper coating depends on the composition of the plating bath. Hu et al.¹⁶ found that in a pyrophosphate-based alkaline bath, the addition of glycerol resulted in an increase in the size of the crystalline grains and a decrease in the microstrain values of the copper coating.

The effect of microstrain on coating characteristics depends on the nature of the microstrain. The introduction of stress of a compressive nature should increase the corrosion resistance of the coating due to the removal of micro-cavities or pores with the application of compressive stress³³. It was found³⁴ that the addition of saccharin to the deposition bath increased the corrosion resistance of a Ni coating, this effect was attributed to the increase in the compression strain caused by the addition of this additive. On the other hand, it has been found that the increase in tensile strain results in a decrease in the coating corrosion resistance. The increase in tensile strain can cause microcracks that damage the coating as the roughness increases and corrosion resistance decreases³⁵. However, it is not clear how the increase in tensile microstrain can affect the corrosion resistance of the copper deposit analyzed in the present work. It is necessary to carry out additional measures in future work, such as porosity measurements.

3.3. Effect of glycerol addition on deposition current efficiency of Cu coating

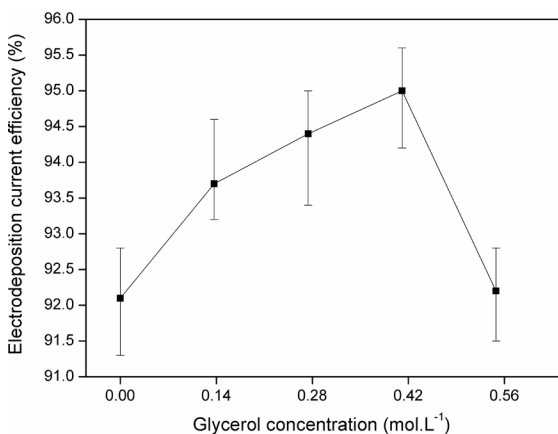
Figure 4 shows the current efficiency values of the Cu coating electrodeposition process obtained in the absence and presence of different glycerol contents. Table 6 lists the average values of energy consumed during the electrodeposition process.

The results reported in Figure 4 show that the current efficiency of the Cu coating electrodeposition process increases with the addition of glycerol up to a concentration of 0.42 mol·L⁻¹, reaching a maximum value at this concentration. Higher current efficiency results in a lower energy consumption of the electroplating process. Table 6 shows that the lowest energy consumption occurs with the addition of 0.42 mol·L⁻¹ of glycerol.

The increased efficiency of the deposition current caused by the addition of glycerol has also been observed in the deposition of Zn-Ni¹⁵ and Ni³⁶ coatings. However, it has been found that in the deposition of Zn from an acid bath¹¹ and copper from a pyrophosphate-based bath¹², the addition of glycerol reduces the deposition efficiency. These results therefore show that the effect of glycerol on the deposition current efficiency depends on the nature of the deposition bath.

Table 6. Energy consumption average values in the absence and presence of different glycerol concentrations.

Glycerol concentration (mol·L ⁻¹)	Energy consumption (kWh·ton ⁻¹)		
	Max.	Min.	Aver.
0	21906	21552	21720
0.14	21459	21142	21343
0.28	21413	21053	21191
0.42	21231	20921	21044
0.56	21858	21529	21697

**Figure 4.** Effect of glycerol addition on current efficiency of Cu coating.

The effect of the addition of an additive on the efficiency of galvanostatic deposition has been related to several factors including the hydrogen evolution reaction, the viscosity of the deposition bath, the complexation of metal ions, the potential at which the deposition occurs, and the adsorption of glycerol on the surface of the cathode. The decrease in the electrical conductivity of the deposition bath with the addition of glycerol, as observed in Table 1, tends to inhibit the mass transport of Cu²⁺ ions, which favors the decrease in the efficiency of the deposition current. Therefore, in the present work, the increase in current efficiency caused by the addition of glycerol indicates that another factor predominated in the effect of glycerol on decreasing electrical conductivity.

The hydrogen evolution reaction occurs simultaneously with the Cu reduction reaction and therefore the inhibition of the hydrogen evolution reaction favors the increase in the deposition current efficiency. Oliveira et al.³⁷ reported that the addition of glycerol in the nickel deposition bath increased the deposition efficiency through the inhibition of the hydrogen evolution in the platinum substrate. This is attributed to the reaction of glycerol with boric acid forming a boric-polyalcohol complex on the surface of the platinum (Pt) substrate, thus decreasing the active area of hydrogen adsorption and consequently its evolution. However, as observed by Sekar et al.¹⁷, the addition of glycerol in an alkaline bath based on pyrophosphate inhibits the evolution of hydrogen, but does not increase the current efficiency of copper deposition. This is related to the high current efficiency of the Cu deposition in this solution, and the

inhibition of hydrogen evolution was not enough to increase the deposition efficiency.

In the present work, it is possible that the presence of glycerol led to a level of inhibition of hydrogen evolution sufficient to increase the efficiency of the deposition current. The inhibition of the hydrogen evolution reaction caused by the addition of glycerol may be related to the reduction of defects present in the coating, such as grooves and cavities³⁸. Therefore, as H^+ ions are likely to lodge in these defects, the presence of glycerol may result in the inhibition of the hydrogen evolution reaction.

The decrease in current efficiency with the increase in the glycerol content from $0.42 \text{ mol}\cdot\text{L}^{-1}$ to $0.56 \text{ mol}\cdot\text{L}^{-1}$ may be related to the possible presence of cracks in the coating obtained at this concentration, which act as adsorption sites for H^+ , thus favoring the hydrogen evolution reaction.

3.3. Effect of glycerol addition on the corrosion resistance of Cu coating

Figure 5 shows the corrosion rate obtained through mass loss tests in the 2 M NaCl solution of Cu coating obtained in the absence and presence of different concentrations of glycerol. These results show that corrosion rate decreases with the addition of glycerol. The corrosion rate decreases with increasing glycerol concentration up to 0.42 g/L . Therefore, these results indicate that there is an optimal concentration of glycerol, at which the corrosion resistance of the Cu coating is maximized.

The potentiodynamic polarization curves, E vs. $\log i$, are shown in Figure 6. From these curves we obtained the corrosion potential, E_{cor} , listed in Table 7, and the corrosion current density, i_{cor} , shown in Figure 7. Figure 8 shows the resistance R_p values from potentiodynamic polarization curves, E vs. i .

The polarization curves in Figure 6 show that with the addition of glycerol there is a decrease in the current density in the anode region. This indicates a lower dissolution of the Cu coating with the addition of glycerol, which is less intense with the addition of $0.42 \text{ mol}\cdot\text{L}^{-1}$ of glycerol.

Table 7 shows that the coating obtained in the absence of glycerol is not the one with the lowest E_{cor} , despite having a higher corrosion resistance than a coating containing glycerol according to the mass loss tests. In several works involving metallic coatings, it has been observed that a deposit with the highest E_{cor} exhibits a lower rate of corrosion in NaCl solution. This was observed, for example, in a study³⁸ on Zn-Ni coatings obtained using baths of different compositions and in a study on the effect of the addition of different concentrations of Al_2O_3 on the corrosion resistance of the Zn-Ni coating³⁹. On the other hand, it has also been found that the addition of nanoparticles, such as SiO_2 and CeO_2 , decreases the corrosion rate of Zn-Ni coating, however, slightly decreases the E_{cor} ⁴⁰. In fact, the E_{cor} , which is a dynamic value, can show the corrosion tendency, but it is not possible to say that a higher E_{cor} necessarily indicates a lower corrosion rate, which is a kinetic value⁴¹. For example, the corrosion potential does not reflect the actual effect of the presence of the corrosion product on the corrosion rate.

Figures 7 and 8 show, respectively, that the i_{cor} decreases and the R_p increases with glycerol addition. These figures

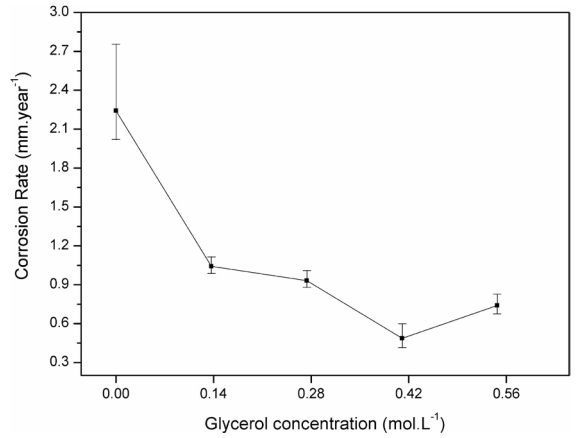


Figure 5. Corrosion rate in the 2M NaCl solution of Cu coatings obtained without and in the presence of different concentrations of glycerol.

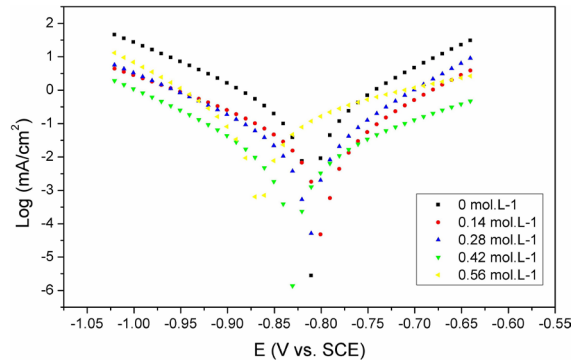


Figure 6. Potentiodynamic polarization curves in the 2 M NaCl solution of copper coatings obtained in the absence and presence of different concentrations of glycerol.

Table 7. Corrosion potential in the 2 M NaCl solution of copper coatings obtained in the absence and presence of different concentrations of glycerol.

Glycerol concentration (mol.L ⁻¹)	E_{cor} (mV _{SCE})		
	Min.	Max.	Med.
0	- 880.97	- 706.05	- 799.34
0.14	- 798.43	- 796.69	- 797.45
0.28	- 815.12	- 795.95	- 804.78
0.42	- 900.46	- 652.42	- 772.07
0.56	- 964.38	- 949.34	- 957.42

show that the i_{cor} is minimal and the R_p is maximum at the concentration of 0.42 mol/L of glycerol. Therefore, considering that a lower i_{cor} and a higher R_p indicate a higher corrosion resistance, the results shown in Figures 7 and 8 show that the addition of glycerol increases the corrosion resistance of the Cu coating. These results are consistent with the mass loss tests indicating that there is an optimal concentration of glycerol, around 0.42 mol/L , at which the corrosion resistance of the Cu coating is maximized. However, the evaluation

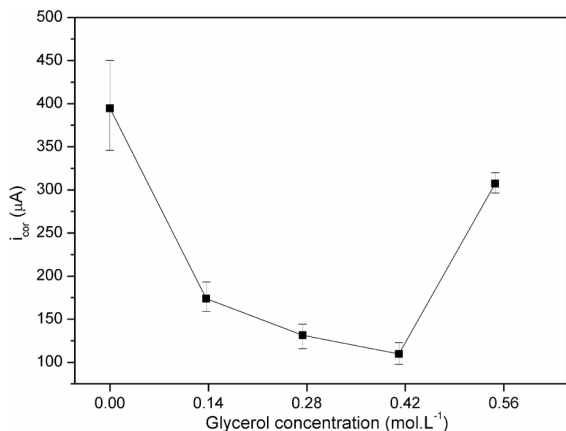


Figure 7. Corrosion current variation of copper deposits with glycerol variation, obtained from a 2 M NaCl solution.

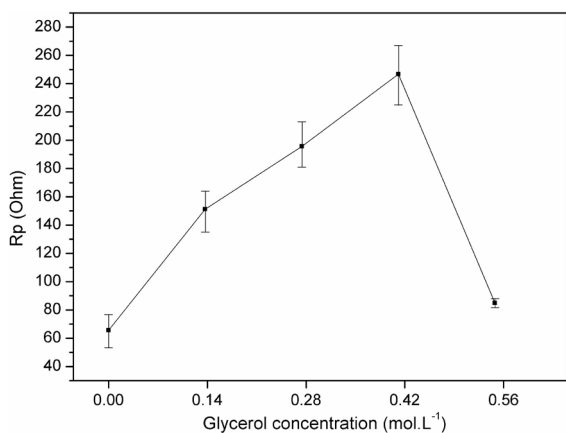


Figure 8. Polarization resistance variation of copper deposits with glycerol variation, obtained from a 2 M NaCl solution.

of corrosion resistance through the mass loss test indicates that the corrosion resistance of the coating obtained in the presence of 0.56 mol·L⁻¹ of glycerol is close to the coating obtained in the presence of 0.42 mol·L⁻¹ of glycerol, while the measurements of i_{cor} and R_p show that the coating obtained in the presence of this concentration has a significantly higher corrosion resistance than the coating obtained in the presence of 0.56 mol·L⁻¹. This is probably related to a limitation of the mass loss test, which demonstrates the difficulty of completely eliminating the corrosion product from the sample after immersion in the corrosive solution. This difficulty occurs mainly in samples that undergo more intense corrosion, such as the sample obtained in the presence of 0.56 mol·L⁻¹ of glycerol, which presents a greater amount of corrosion products.

The increase in corrosion resistance of the copper coating in the NaCl solution due to the addition of glycerol in the deposition acid bath is related to changes in the morphology and structure of the deposit. The formation of smoother and more compact deposits with the addition of glycerol reduces the surface area in contact with the aggressive solution, which favored the increase in corrosion resistance.

The grain refining caused by the addition of glycerol, in addition to favoring the presence of a smoother surface, also promotes a more homogeneous current distribution in the coating, which favors corrosion resistance. As the grain size decreases, the grain boundary area and the number of triple points of intersection of the boundaries increase. Therefore, considering that these sites act as preferential corrosion sites, it has been proposed⁴² that the increased presence of these sites implies a greater dispersion of the corrosion current density. Increased corrosion resistance due to a more evenly distributed corrosion current is attributed to the occurrence of a smaller cathode/anode surface ratio against localized corrosion⁴³. However, when the fraction of triple junction volume is very high, which occurs in nanocrystalline grains below a certain size, the increase of this defect favored the corrosion. A possible explanation for this behavior is that atomic movement is facilitated, as it is mainly related to the triple junction and not to the grain boundary, which favors corrosion⁴⁴.

It has been found⁴⁴ for Ni and Ni-W coatings that with the refining of the nanometric grains below 10 nm, an increase in the corrosion rate in the NaCl solution begins to occur, which is attributed to the presence of a fraction of triple junction. However, in the present work it is not clear that the decrease in corrosion resistance with the increase of the glycerol content to 0.56 mol·L⁻¹ is related to the increase in the triple junction because the average dimension of the crystallites of the coating containing this is 25.3 nm.

The increase in the corrosion resistance of Cu coating with the increase of glycerol concentration up to 0.42 mol·L⁻¹ is related to the occurrence of a smoother coating with smaller grains. On the other hand, the decrease in corrosion resistance caused by the addition of 0.56 mol·L⁻¹ of glycerol may be related to the occurrence of a higher roughness, as observed in Table 4. This higher roughness, probably caused by the higher level of coating tension, increases the surface area resulting in less corrosion resistance.

The higher corrosion resistance in the Cu coating obtained in the presence of 0.42 mol·L⁻¹ is consistent with the results that indicate a higher current efficiency at this concentration. This is due to the presence of a smoother and more compact coating that occurs at this concentration which implies fewer defects that absorb H⁺, with a consequent decrease in hydrogen evolution.

4. Conclusion

In the present work Cu coatings were obtained using an acid sulphate solution in the absence and in the presence of different amounts of glycerol. Measurements from SEM and X-ray diffraction show that the addition of glycerol to the bath deposition decreases the grain and crystallite sizes, and this effect is more accentuated with certain amounts of glycerol. The addition of glycerol reduced the grain size of copper electrodeposits by 28%, promoting more compact phases of copper deposits. With the addition of 0.56 mol·L⁻¹ of glycerol the population density of the grains (grains/µm²) increased from 0.3195 grains/µm² to 0.6082 grains/µm², and it was observed that there were around one hundred crystallites in each grain. Nanometer copper crystallites with an average of 30 nm were obtained.

The nature of the deformation present in the copper coatings analyzed in this work is tensile and the addition of glycerol increases this tension. The texture coefficient (T_c) values indicate that the copper coating deposited both in the absence and in the presence of glycerol has as preferential orientation: the plane (220). However, there is no clear trend as to how the addition of glycerol affects T_c .

The addition of glycerol makes the Cu coating more compact and reduces its roughness, with a minimum roughness corresponding to a concentration of $0.42 \text{ mol}\cdot\text{L}^{-1}$ of glycerol. The increase in roughness with the increase in the glycerol content to $0.56 \text{ mol}\cdot\text{L}^{-1}$ may be related to the higher level of tension of the coating obtained at this concentration.

Furthermore, the current efficiency of the Cu coating electrodeposition process increased with the addition of glycerol up to a concentration of $0.42 \text{ mol}\cdot\text{L}^{-1}$, reaching a maximum value at this concentration.

Electrochemical and mass loss tests showed that the addition of glycerol increased the corrosion resistance of the Cu coating by approximately 96%, and that there is an optimal concentration of glycerol, around $0.42 \text{ mol}\cdot\text{L}^{-1}$, in which the corrosion resistance of the Cu coating is maximized. This is related to the effect of glycerol on the roughness and refining of grains in the Cu coating.

Traditional solutions in industry mostly involve the use of cyanides, however, the use of glycerol in the electrodeposition bath can be considered a promising sustainable alternative to mitigate environmental damage and promote safety. A Brazilian patent has been granted with such a purpose⁴⁵.

5. Acknowledgments

The authors are grateful to the Bahia State Research Support Fund (FAPESB) and CAPES for financial support for completing that work. Special thanks to the teachers of the Department of Science and Technology of Materials and laboratories of the Institute of Chemistry and Nuclear Physics Institute of UFBA for their ongoing collaboration in conducting the tests.

6. Reference

- Schlesinger M, Paunovic M, editors. Modern electroplating. Hoboken: John Wiley & Sons; 2010.
- Dash R, Balomajumder C, Kumar A. Removal of cyanide from water and wastewater using granular activated carbon. *Chem Eng J*. 2009;146(3):408-13.
- Lowenheim FA, editor. Modern electroplating. 5th ed. Hoboken: John Wiley and Sons; 2014.
- Dini JW, Snyder DD, editors. Modern electroplating. 5th ed. Hoboken: Wiley Online Library; 2011.
- Moraes ACMD, Siqueira JLP, Barbosa LL, Carlos IA. Voltammetric study of the influence of benzotriazole on copper deposition from a sulphuric plating bath. *J Appl Electrochem*. 2009;39(3):369-75.
- Watkowski J, editor. Electroplating in printed circuits handbook. 6th ed. New York: McGraw-Hill; 2008.
- Grandell L, Thorenz A. Silver supply risk analysis for the solar sector. *Renew Energy*. 2014;69:157-65.
- Groover MP, editor. Fundamental of modern manufacturing - materials, processes and systems. 4th ed. Hoboken: John Wiley @ Sons; 2010.
- Safizadeh F, Lafronta AM, Ghalia E, Houlachi G. Monitoring the quality of copper deposition by statistical and frequency analyses of electrochemical noise. *Hydrometallurgy*. 2010;100(3-4):87-94.
- Quinet M, Lallemand F, Ricq L, Hihn JY, Delobelle P, Arnould C, et al. Influence of organic additives on the initial stages of copper electrodeposition on polycrystalline platinum. *Electrochim Acta*. 2009;(54):1529-36.
- Kim H C, Kim M J, Lim T, Park K J, Kim H K, Choe S, Kim S K, Kim JJ. Effects of nitrogen atoms of benzotriazole and its derivatives on the properties of electrodeposited Cu films. *Thin Solids film*. 2014;5050:421-7.
- Tantavichet N, Pritzker M. Copper electrodeposition in sulphate solutions in the presence of benzotriazole. *J Appl Electrochem*. 2006;36(1):49-61.
- Vas'ko V, Tabakovic I, Riemer S, Kief M. Effect of organic additives on structure, resistivity, and room-temperature recrystallization of electrodeposited copper. *Microelectron Eng*. 2004;75(1):71-7.
- Jesus MDD, Rovere CAD, de Andrade Lima LR, Ribeiro DV, Souza CAC. Glycerol effect on the corrosion resistance and electrodeposition conditions in a zinc electroplating process. *Mater Res-ibero-AM J*. 2019;22(4):1-13.
- Pedroza GAG, Sousa CAC, Carlos IA, de Andrade Lima LR. Evaluation of the effect of deposition bath glycerol content on zinc-nickel electrodeposits on carbon steel. *Surf Coat Tech*. 2012;206:2927-32.
- Hu J, Li Q, An M, Zhang J, Yang P. Influence of glycerol on copper electrodeposition from pyrophosphate bath: nucleation mechanism and performance characterization. *J Electrochem Soc*. 2018;165(11):D585-94.
- Sekar R, Jagadesh KK, Ramesh Babu GNK. Electrodeposition and characterisation of copper deposits from non-cyanide electrolytes. *Surf Eng*. 2015;31(6):433-8.
- De Almeida MRH, Carlos IA, Barbosa LL, Carlos RM, Lima-Neto BS, Pallone EMJA. Voltammetric and morphological characterization of copper electrodeposition from non-cyanide electrolyte. *J Appl Electrochem*. 2002;32:763-73.
- Schneider CA, Rasband WS, Eliceiri KW. NIH Image to ImageJ: 25 years of image analysis. *Nat Methods*. 2012;9:671-5.
- Franco LA, Sinarua A. 3D surface parameters (ISO 25178-2): Actual meaning of Spk and its relationship to Vmp. *Precis Eng*. 2015;40:106-11.
- Ramgir NS, Kyuhwang Y, Mulla IS, Chang JS. Effect of particle size and strain in nanocrystalline SnO₂ according to doping concentration of ruthenium. *Solid State Sci*. 2006;8(3-4):359-62.
- Hammond C. The basis of crystallography and diffraction. 3rd ed. Oxford: Oxford University Press; 2009.
- Nath D, Singh F, Das R. X-ray diffraction analysis by Williamson-Hall, Halder-Wagner and size-strain plot methods of CdSe nanoparticles- a comparative study. *Mater Chem Phys*. 2020;239:122021-30.
- Yusoff AHM, Salimi MN, Jamlos MF. Dependence of lattice strain of magnetite nanoparticles on precipitation temperature and pH of solution. *J Phys Conf Ser*. 2017;908:1-6.
- Sarkar S, Das R. Determination of structural elements of synthesized silver nano-hexagon from X-ray diffraction analysis. *Indian J Pure Appl Phys*. 2018;56:765-72.
- Soares ME, Souza C A C, Kuri SE. Corrosion resistance of a Zn-Ni electrodeposited alloy obtained with a controlled electrolyte flow and gelatin additive. *Surf Coat Tech*. 2006;201(6):2953-9.
- Faraday M. On electrical decomposition. *Philos TR Soc*. 1834;1834(124):77-122.
- Lins V F C, Castro MMC, Araujo CR, Oliveira DB. Effect of nickel and magnesium on zinc electrowinning using sulfate solutions. *Braz J Chem Eng*. 2011;28(3):475-82.

29. ASTM: American Society for Testing and Materials. ASTM G31-72: Standard Practice for Laboratory Immersion Corrosion Testing of Metals. West Conshohocken: ASTM; 2004.
30. Stern M, Geary AL. Electrochemical polarization: I. A theoretical analysis of the shape of polarization curves. *J Electrochem Soc.* 1957;104:56-63.
31. Das S, Jena S, Banthia S, Mitra A, Das S, Das K. Novel pulse potentiostatic electrodeposition route for obtaining pure intermetallic Cu₂Zn₈-CuZn composite coating using glycerol-NaOH based electrolyte with advanced scratch resistance and anti-corrosive properties. *J Alloys Compd.* 2019;795:770-9.
32. Hamid AZ, Aal A. New environmentally friendly noncyanide alkaline electrolyte for copper electroplating. *Surf Coat Tech.* 2009;203(10):1360-5.
33. Sekar R. Synergistic effect of additives on electrodeposition of copper from cyanide-free electrolytes and its structural and morphological characteristics. *T Nonferr Metal Soc.* 2017;27(7):1665-76.
34. Montero-Ocampo C, Veleza L. Effect of cold reduction on corrosion of carbon steel in aerated 3% sodium chloride. *Corros.* 2002;58(7):601-7.
35. Mishara R, Balasubramaniam R. Effect of nanocrystalline grain size on the electrochemical and corrosion behavior of nickel. *Corros Sci.* 2004;46(12):3019-29.
36. Gürbüz E, Aydın R, Şahin BA. Study of the influences of transition metal (Mn,Ni) co-doping on the morphological, structural and optical properties of nanostructured CdO films. *J Mater Sci Mater Electron.* 2018;29:1823-31.
37. Oliveira EM, Finazzi GA, Carlos IA. Influence of glycerol, mannitol and sorbitol on electrodeposition of nickel from a Watts bath and on the nickel film morphology. *Surf Coat Tech.* 2006;200:5978-85.
38. Sriraman KR, Brahimi S, Szpunar JA, Osborne JH, Yue S. Characterization of corrosion resistance of electrodeposited Zn-Ni Zn and Cd coatings. *Electrochim Acta.* 2013;105:314-23.
39. Blejan D, Muresan LM. Corrosion behavior of Zn-Ni-Al₂O₃ nanocomposite coatings obtained by electrodeposition from alkaline electrolytes. *Werkst Korros.* 2012;63:1-6.
40. Xiang T, Zhang M, Li C, Dong C, Yang L, Chan W. CeO₂ modified SiO₂ acted as additive in electrodeposition of Zn-Ni alloy coating with enhanced corrosion resistance. *J Alloys Compd.* 2018;736:62-70.
41. Zhang XG. Corrosion and electrochemistry of zinc. Boston: Springer; 1996. Corrosion potential and corrosion current.
42. Gu CG, Lian JS, He JG, Jiang ZH, Jiang Q. High corrosion-resistance nanocrystalline Ni coating on AZ91D magnesium alloy. *Surf Coat Tech.* 2006;200:5413-8.
43. Azar MMK, Guptapeh HS, Rezaei M. Evaluation of corrosion protection performance of electroplated zinc and zinc-graphene oxide nanocomposite coatings in air saturated 3.5 wt. % NaCl solution. *Colloids Surf A Physicochem Eng Asp.* 2020;601:12501.
44. Wasekar NP. The influence of grain size and triple junctions on corrosion behavior of nanocrystalline Ni and Ni-W alloy. *Scr Mater.* 2022;213:114604.
45. Barbosa RS, Souza CC, Nascimento MLF. Copper electrodeposition method from acid solution and improvement in coating metals using organic glycerol-based additives. Brasil patent, BR 1020190260840. 2019, Dec 10.

Supplementary material

The following online material is available for this article:
Appendix